LETTERS

Calcium flickers steer cell migration

Chaoliang Wei[1], Xianhua Wang[1], Min Chen[1], Kunfu Ouyang[1], Long-Sheng Song[2] & Heping Cheng[1]

Directional movement is a property common to all cell types during development and is critical to tissue remodelling and regeneration after damage[1–3]. In migrating cells, calcium has a multifunctional role in directional sensing, cytoskeleton redistribution, traction force generation, and relocation of focal adhesions[1,4–7]. Here we visualize high-calcium microdomains ('calcium flickers') and their patterned activation in migrating human embryonic lung fibroblasts. Calcium flicker activity is dually coupled to membrane tension (by means of TRPM7, a stretch-activated Ca^{2+}-permeant channel of the transient receptor potential superfamily[8]) and chemoattractant signal transduction (by means of type 2 inositol-1,4,5-trisphosphate receptors). Interestingly, calcium flickers are most active at the leading lamella of migrating cells, displaying a 4:1 front-to-rear polarization opposite to the global calcium gradient[6]. When exposed to a platelet-derived growth factor gradient perpendicular to cell movement, asymmetric calcium flicker activity develops across the lamella and promotes the turning of migrating fibroblasts. These findings show how the exquisite spatiotemporal organization of calcium microdomains can orchestrate complex cellular processes such as cell migration.

In addition to extracellular chemoattractant stimuli, directional cell movement depends on an intracellular calcium signal that is well-organized in space, time and concentration[6,7,9]. Over a decade ago, it was shown that intracellular calcium displays a rear-to-front gradient, with the lowest concentration at the front of a migrating cell[6]. However, this observation seems to be paradoxical, because the leading lamella—the signalling and motility centre of a migrating cell—contains numerous effector proteins that require high levels of calcium for activation[10–13]. Although transient increases of calcium concentration have recently been observed in migrating cells, they are infrequent and mainly localized to the tail of the cell, and are thought to facilitate intermittent rear retraction[7]. Biochemical studies indicate that calcium entry is required to maintain ruffling structure, actin polymerization and the phosphatidylinositol-3,4,5-trisphosphate (PtdIns(3,4,5)P_3) signalling at the leading edge of macrophages[14]. So far, it has been perplexing how calcium regulates lamella dynamics during cell migration.

Using human embryonic lung fibroblasts (WI-38) as a model, we characterized the spatiotemporal organization of intracellular calcium signals with the aid of real-time confocal microscopy. In migrating WI-38 fibroblasts that overtly displayed leading and trailing edges, we detected a shallow decreasing gradient of global calcium concentration (indexed by the Fluo-4 to Fura red fluorescence ratio) that ran from the rear to the front (Fig. 1c, d), in agreement with previous findings[6,9]. Surprisingly, we found that discrete, local and short-lived high-calcium microdomains or 'calcium flickers', analogous to calcium sparks and puffs[15], occurred against a quiescent background (Supplementary Video). High-resolution linescan imaging revealed that the flickers occurred at a nearly constant rate of 1.92 ± 0.21 Hz per 100-μm linescan ($n = 18$; Fig. 1c). Individual events rapidly rose to about double the Fluo-4 fluorescence ($\Delta F/F_o = 1.16 \pm 0.02$, $n = 1{,}071$), lasted variably from 10 ms to 4 s, and were confined to an area 5.27 ± 0.05 μm in diameter (Fig. 1c). Importantly, calcium flickers were abundant at the leading lamella (Fig. 1a), including in motile lamellipodia (Fig. 1b), but were sharply reduced elsewhere, resulting in an approximately 4:1 front-to-rear polarization (Fig. 1d) that was opposite to the aforementioned global calcium gradient. Polarization of flicker activity was common to fibroblasts undergoing migration, but was not seen in stationary

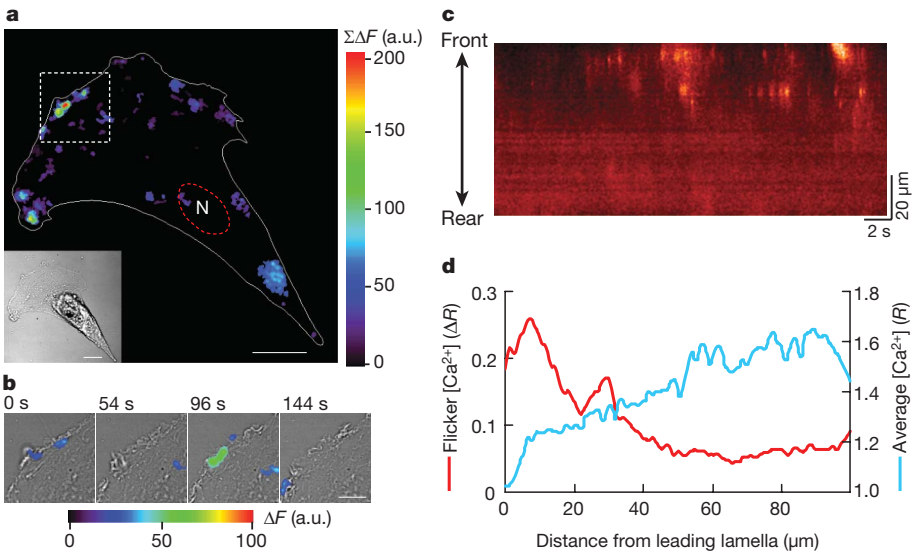

Figure 1 | Calcium flickers in migrating fibroblasts. **a**, Calcium flickers. In a polarized WI-38 fibroblast (inset), local calcium increases ($\Sigma\Delta F$) were summed over 30 consecutive images acquired at 6-s intervals. 'N' marks the nucleus. Scale bars, 15 μm. **b**, Calcium flickers (colour overlay) in motile lamellipodia (box in **a**). Scale bar, 5 μm; a.u., arbitrary units. **c**, Polarization of calcium flicker activity. The image consists of 10,000 front-to-rear linescans, expressed as the ratio between Fluo-4 and Fura red fluorescence (R). **d**, Opposing gradients of calcium flicker activity (ΔR) and global calcium (R, inclusive of flicker activity). Similar results were obtained in eight cells.

[1]Institute of Molecular Medicine, State Key Laboratory of Biomembrane and Membrane Biotechnology, Peking University, Beijing 100871, China. [2]Department of Internal Medicine, Division of Cardiovascular Medicine, University of Iowa Carver College of Medicine, Iowa City, Iowa 52242, USA.

©2009 Macmillan Publishers Limited. All rights reserved

fibroblasts lacking morphological polarity and displaying a lower flicker incidence (0.57 ± 0.10 Hz per 100-μm linescan, $n = 12$, $P < 0.05$ versus migrating cells; Supplementary Fig. 1). Thus, flickers represent a distinctive, heretofore unappreciated, modality of calcium signalling in migrating fibroblasts. Similar flickers were also evident in rat neonatal cardiac fibroblasts and 3T3-Swiss albino mouse embryonic fibroblasts (Supplementary Fig. 2).

In search of the molecular basis of calcium flickers, we showed that calcium influx through the stretch-activated cation channel (SACC) was obligatory. Application of Ca^{2+}-free medium containing 5 mM EGTA or streptomycin (200 μM), a SACC blocker[16], immediately abolished flicker activity in WI-38 fibroblasts (Fig. 2a). On average, the signal mass of calcium flickers (space–time integral of the flicker signal) decreased by $98.3 \pm 0.8\%$ (EGTA; $n = 9$, $P < 0.01$ versus control) or $93.1 \pm 1.3\%$ (streptomycin; $n = 6$, $P < 0.01$ versus control). Likewise, Gd^{3+} (200 μM), a non-specific SACC blocker[16], diminished the signal mass by $91.9 \pm 1.2\%$ ($n = 6$, $P < 0.01$ versus control). To determine whether mechanical forces can directly trigger flickers, we showed that shear stress applied to the front of migrating fibroblasts immediately evoked a flurry of flicker activity (Fig. 2e). In a different approach, relaxing or stretching the cell by pushing or pulling the flexible substrate (with a needle tip) suppressed or enhanced the flicker activity, respectively (Supplementary Fig. 3). Under cell-attached patch-clamp conditions[17], sudden application of negative pressure (~40 mm Hg) elicited bursting single-channel activity, whereas simultaneous confocal imaging visualized corresponding flicker-like events beneath the patch membrane (Fig. 2b). These results indicate that calcium flickers are triggered by calcium influx through SACCs.

SACCs belong to the transient receptor potential (TRP) ion channel superfamily. In mammals, about eight TRP channels in four subfamilies are thought to be sensitive to mechanical forces while being calcium-permeable[8]. Of these, there were relatively high *TRPM7*, *TRPC6*, *TRPV2* and *PKD2* (also known as PC2 or TRPP2) messenger RNA levels in WI-38 fibroblasts (Supplementary Fig. 4). Using RNA interference (RNAi), we found that calcium flickers were virtually abolished by ~75% knockdown of *TRPM7*, but not by that of the other three TRP channels (Fig. 2c, d and Supplementary Fig. 5). More importantly, similar shear stress was unable to evoke flickers in *TRPM7* knockdown cells, which displayed rare basal flicker activity (Fig. 2e). These data pinpointed TRPM7 as the specific SACC responsible for transducing mechanical signals into calcium flickers. A characteristic of TRPM7 is its sensitivity to inhibition by Mg^{2+} in addition to Gd^{3+} (ref. 18). Increasing extracellular Mg^{2+} from 1.0 mM to 10 mM largely abolished calcium flickers, whereas removing it enhanced flicker production (Supplementary Fig. 6). Thus, TRPM7 acts as the mechanical sensor, the calcium flicker igniter and the mechanochemical transducer in fibroblasts, revealing a previously unknown role of this SACC in the regulation of cell migration (see below).

Because calcium release from the endoplasmic reticulum amplifies calcium influxes by means of the calcium-induced calcium release mechanism[15], we next investigated whether endoplasmic reticulum calcium release participates in calcium flicker production. Inhibition of endoplasmic reticulum calcium recycling with the Ca^{2+} ATPase inhibitor thapsigargin (5 μM, 20 min incubation, after recession of the initial calcium transient) halved flicker amplitude without affecting flicker probability (Fig. 3a, c). Similar results were obtained by inhibiting the inositol-1,4,5-trisphosphate ($Ins(1,4,5)P_3$) receptor ($Ins(1,4,5)P_3R$) with xestospongin C (5 μM), whereas $Ins(1,4,5)P_3$-BM (2 μM), a membrane-permeable ester precursor of $Ins(1,4,5)P_3$ (ref. 19), enhanced the flicker amplitude, and ryanodine receptor inhibition (ryanodine, 25 μM) had no significant effect (Fig. 3a, c). Quantitative real-time polymerase chain reaction (PCR) results showed that type 2 $Ins(1,4,5)P_3R$ ($Ins(1,4,5)P_3R2$) and type 3 $Ins(1,4,5)P_3R$ ($Ins(1,4,5)P_3R3$) are the primary $Ins(1,4,5)P_3R$ isoforms expressed in WI-38 fibroblasts (Supplementary Fig. 7). In contrast to TRPM7, RNA interference knockdown of the gene encoding $Ins(1,4,5)P_3R2$ (~80%), but not that encoding $Ins(1,4,5)P_3R3$ (~60%), significantly decreased flicker amplitude but failed to alter flicker probability (Fig. 3b, c). This $Ins(1,4,5)P_3R$ isoform specificity is consistent with the fact that $Ins(1,4,5)P_3R2$ is more sensitive to $Ins(1,4,5)P_3$ and displays little calcium-dependent inactivation[20]. Taken these findings together, we concluded that calcium entry by means of TRPM7 is locally amplified by calcium release through $Ins(1,4,5)P_3R2$ in the event of a calcium flicker. Coupling $Ins(1,4,5)P_3R2$ to TRPM7 would enable flicker activity to decode $Ins(1,4,5)P_3$-linked chemoattractant signal transduction.

Given the role of TRPM7 as a mechanical sensor and a calcium flicker igniter, we anticipated that flicker activity would be coupled to

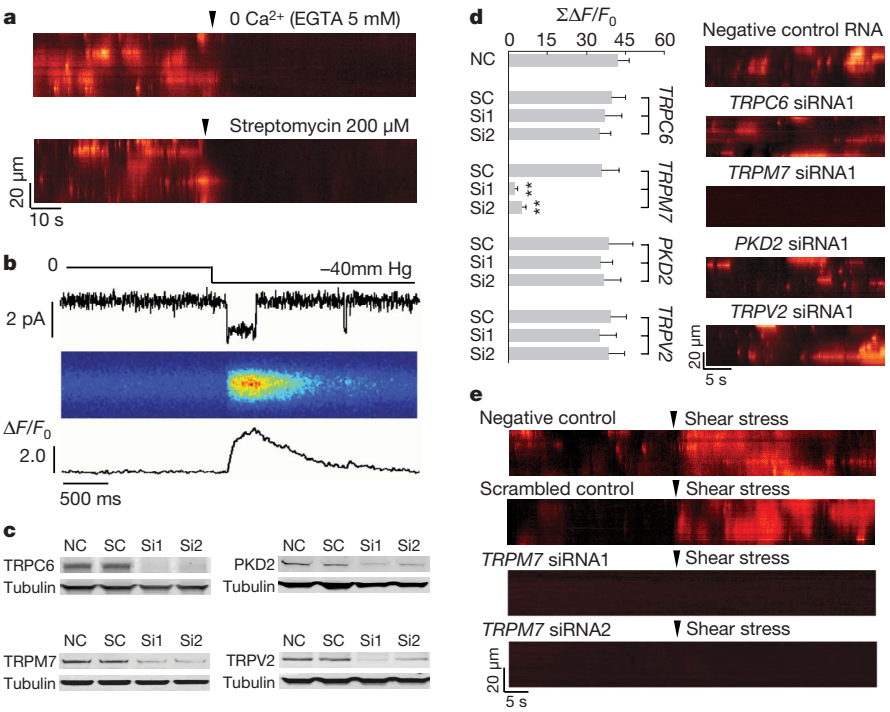

Figure 2 | Triggering calcium flickers by TRPM7. **a**, Abolition of calcium flickers by streptomycin or removal of external calcium. **b**, Visualization of calcium entry through single SACCs. From top to bottom: suction through the patch pipette; single-channel currents; and linescan image and line plot of local calcium transients. **c**, RNAi knockdown of *TRPC6*, *TRPM7*, *TRPV2* and *PKD2* assayed by western blotting. NC, negative control RNA; SC, scrambled control RNA; Si1 and Si2, different siRNA sequences (see Supplementary Table 2). **d**, Knockdown of *TRPM7*, but not *TRPC6*, *TRPV2* or *PKD2*, abolished calcium flickers. Data are expressed as mean and s.e.m.; $n = 12$–21 cells in each group; double asterisk, $P < 0.01$ versus the respective SC. **e**, *TRPM7* knockdown prevented shear-stress-induced calcium flickers.

©2009 Macmillan Publishers Limited. All rights reserved

the migration-associated traction force. Indeed, the map of flicker ignition sites at the front of a cell largely overlapped, although with subtle differences, the matrix of focal adhesions (Fig. 4a and Supplementary Fig. 8), where traction force is created and transmitted[21]. Rapid local application of RGDS (2 mM, 1 min), which contains the RGD sequence that is recognized by integrins[22], enhanced the flicker activity, whereas the control peptide RGES was ineffective (Fig. 4b, c), consistent with the finding that RGDS stimulates calcium transients in neuronal filopodia and growth cones[23]. Disruption of protrusion by transient frontal application of cytochalasin D and inhibition of myosin ATPase by 2,3-butanedione monoxime or (−)blebbistatin[24] both inhibited lamella flicker production (Fig. 4b, c). These lines of evidence support the idea that decoding local membrane tension by flicker activity depends on cytoskeletal and morphological integrity.

Despite the low global calcium concentration, high-calcium microdomains created by mechanical stress in the leading lamella

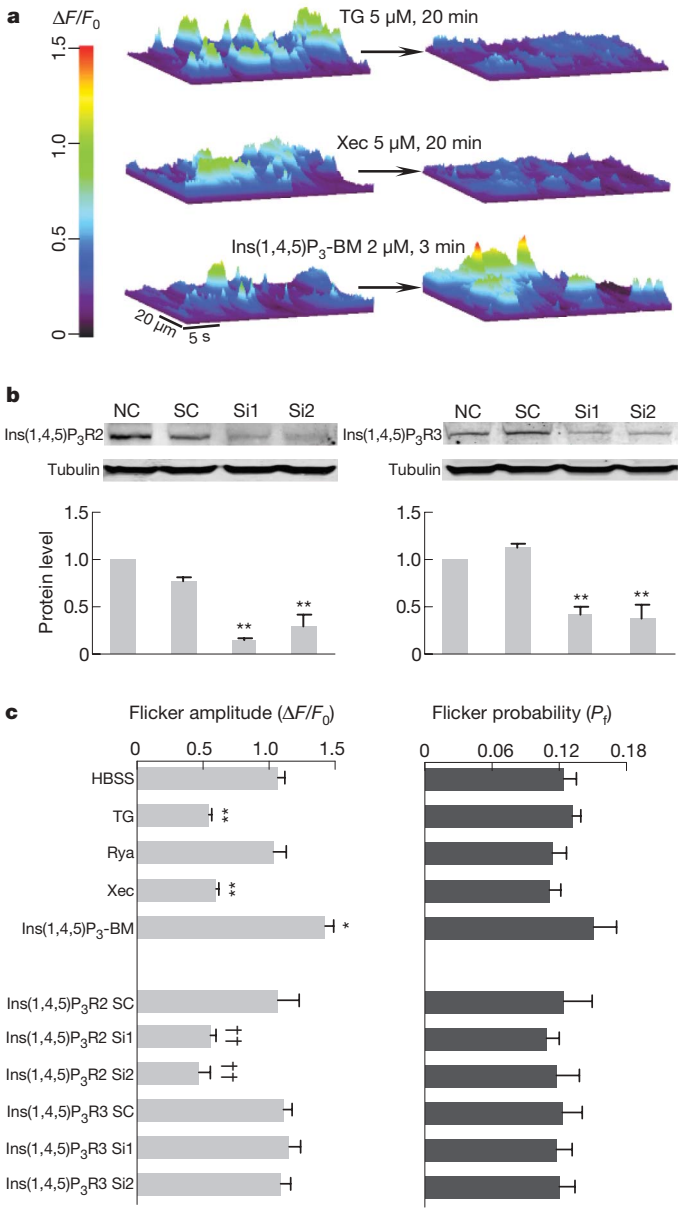

Figure 3 | Amplifying TRPM7 calcium flickers by store calcium release through type 2 Ins(1,4,5)P_3 receptors. **a**, Typical calcium flicker responses to thapsigargin (TG), xestospongin C (Xec) or Ins(1,4,5)P_3-BM. Linescan data of $\Delta F/F_0$ are rendered as surface plots. **b**, Western blotting of Ins(1,4,5)P_3Rs. See Supplementary Table 2 for sequences of negative control (NC), respective scrambled control (SC), Si1 and Si2. Data are expressed as mean and s.e.m. ($n = 3$–4). Double asterisk, $P < 0.01$ versus the respective SC. **c**, Flicker amplitude and probability under different experimental conditions. P_f, fractional time spent in calcium flickers; HBSS, HEPES-buffered saline solution; Rya, ryanodine (25 μM, 15 min). $n = 10$–29; asterisk, $P < 0.05$; double asterisk, $P < 0.01$ versus HBSS; double dagger, $P < 0.01$ versus the respective SC. Note that perturbing the endoplasmic reticulum calcium release mainly altered flicker amplitude without affecting flicker probability.

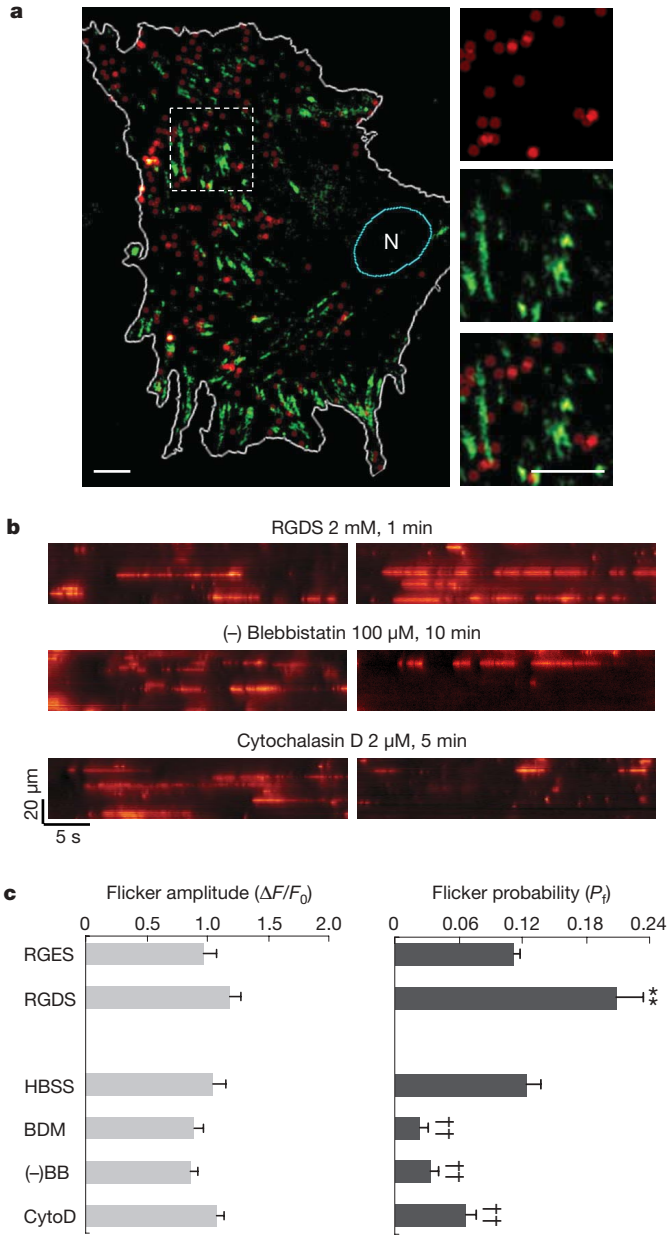

Figure 4 | Traction force generation and calcium flicker activity. **a**, Maps for calcium flicker ignition sites (red dots) and focal adhesions (green). Focal adhesions were visualized by immunostaining for integrin α5 after calcium flicker acquisition. Enlarged views of calcium flickers, focal adhesions and their overlay are shown to the right (top, middle and bottom, respectively). 'N' denotes the nucleus. Scale bar, 8 μm. **b**, Lamella flicker before (left) and after (right) application of compounds that affect traction-force-generating elements. **c**, Statistics of calcium flicker amplitude and probability (P_f). (−)BB, (−)blebbistatin (100 μM); BDM, 2,3-butanedione monoxime (10 mM); cytoD, cytochalasin D; HBSS, HEPES-buffered saline solution. Error bars represent s.e.m.; $n = 10$–19 in each group. Double asterisk, $P < 0.01$ versus RGES; double dagger, $P < 0.01$ versus HBSS. Note that flicker probability rather than amplitude was preferentially altered by varying the traction force, in contrast to the situation shown in Fig. 3.

©2009 Macmillan Publishers Limited. All rights reserved

may activate a multitude of local calcium-dependent events critical to cell polarization and movement, including the PtdIns(3,4,5)P_3 signalling cascade[25,26], a parallel phospholipase A2-mediated signalling mechanism[27], cytoskeleton dynamics such as actin remodelling[10], focal adhesion detachment and relocation, and actin–myosin contraction. Next, we sought to determine the physiological role of calcium flickers in regulating cell migration, particularly turning behaviour that is almost entirely carried out within the leading lamella.

Platelet-derived growth factor (PDGF) is a well known chemoattractant that stimulates fibroblast migration during wound healing[3]. Its intracellular signalling pathways include generating traction force by Rac-dependent protrusion[28] and activation of the phospholipase C–PtdIns(4,5)P_2–Ins(1,4,5)P_3 signalling cascade[29], both convergent on flicker production. When migrating fibroblasts were exposed to uniform PDGF (0.8 nM), increases in both flicker amplitude and probability were accompanied by a decrease in directional persistence (Supplementary Fig. 9), the latter suggesting an enhanced propensity for turning of the cell[30]. When a PDGF gradient was applied in the direction perpendicular to cell movement, migrating fibroblasts no longer moved persistently along the original path; instead, they turned towards the higher PDGF concentration (Fig. 5a). Time-lapse imaging revealed a rapid increase in lamella flicker activity and an accentuated front-to-rear polarization (Fig. 5a). More importantly, a greater flicker signal mass (SM) was found in the portion facing the PDGF source (SM_α) than in the portion further away from the source (SM_β), indicating the development of an asymmetry of flicker activity within the lamella (Fig. 5a). To demonstrate a linkage between lamella flicker asymmetry and turning behaviour, we examined the cumulative difference between SM_α and SM_β ($\Sigma SM_{\alpha-\beta}$) and found that the time course of $\Sigma SM_{\alpha-\beta}$ nearly overlapped with that for the distance travelled in the direction of the PDGF gradient (*y*-distance; Fig. 5b). On average, the correlation coefficient between $\Sigma SM_{\alpha-\beta}$ and *y*-distance was 0.72 in 25 migrating fibroblasts. Hence, patterned flicker activation in the leading lamella may translate directional sense and steer the cell to turn in response to PDGF gradients.

To test this hypothesis further, we showed that impaired PDGF-induced lamella flicker asymmetry or reduction of $\Sigma SM_{\alpha-\beta}$ by streptomycin and *TRPM7* or Ins(1,4,5)P_3R2 knockdown was accompanied by dwindling of the turning angle in a roughly proportional manner (Fig. 5c). Likewise, a robust match between the flicker activity and population chemotaxis was revealed by various pharmacological and molecular interventions including *TRPM7* and Ins(1,4,5)P_3R2 knockdown, and SACC blockade (Fig. 5d and Supplementary Fig. 10). Furthermore, loading EGTA ester to disturb the flicker signal (Supplementary Fig. 11) compromised the turning and chemotaxis abilities (Fig. 5c, d), whereas flicker activation by Ins(1,4,5)P_3-BM enhanced both of these (Fig. 5c, d), suggesting a causal link between calcium flicker activity and fibroblast turning and chemotaxis.

We have demonstrated that calcium flickers arising from TRPM7 and Ins(1,4,5)P_3R2 have an essential role in steering migrating

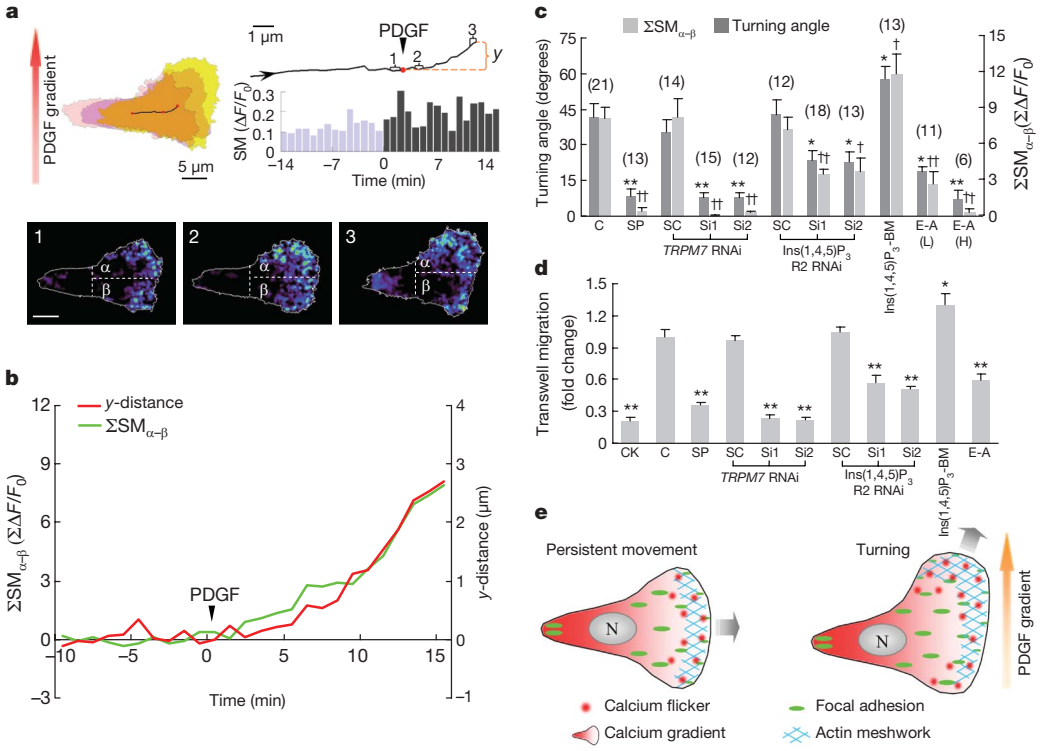

Figure 5 | Calcium flickers steer fibroblast turning. **a**, Asymmetrical lamella flicker activity induced by a PDGF gradient. Top left, contours of the cell border at −14 min (pink), 0 min (purple) and 15 min (yellow). Top right, trajectory of the centre of the cell and time course of calcium flicker production (bar graph). SM, signal mass of calcium flickers within the lamella. Bottom panels: overlays of calcium flickers in 1-min windows (labelled 1–3 in the trajectory above). Dashed lines bisect the leading lamella into upper (α, facing the PDGF source) and lower portions (β). **b**, Correlation between cumulative asymmetric flicker activity ($\Sigma SM_{\alpha-\beta}$) and displacement along the PDGF gradient (*y*-distance). **c**, Relationship between turning angle and $\Sigma SM_{\alpha-\beta}$ (at 15 min). C, control with no treatment; SP, streptomycin, 200 μM; SC, scrambled control; Si1 and Si2, two siRNA duplexes; Ins(1,4,5)P_3-BM, 2 μM; E-A (L), EGTA-AM, 2 μM; E-A (H), EGTA-AM, 20 μM. Data are expressed as mean and s.e.m.; *n* values are shown in parentheses. Asterisk, $P < 0.05$; double asterisk, $P < 0.01$ versus turning angle of control or respective SC; dagger, $P < 0.05$; double dagger, $P < 0.01$ versus $\Sigma SM_{\alpha-\beta}$ of control or respective SC. **d**, Chemotaxis of WI-38 fibroblasts. CK, chemokinesis assay with the same concentration of PDGF-BB on both sides of the well; E-A, EGTA-AM (2 μM). $n = 4$–10; asterisk, $P < 0.05$; double asterisk, $P < 0.01$ versus control or respective SC. **e**, Cartoons of patterned calcium flicker activation in persistently moving (left) and turning (right) fibroblasts. Calcium flicker activity during persistent movement displays a front-to-rear polarization, opposing a rear-to-front global calcium gradient. During turning, calcium flicker activity becomes asymmetric across the leading lamella, in addition to enhanced flicker frequency and accentuated front-to-rear polarization.

©2009 Macmillan Publishers Limited. All rights reserved

fibroblasts. Despite the observation that the global calcium gradient is opposite to the direction of cell migration, high calcium flicker activity would enable activation of calcium signalling cascades amidst a low-calcium background at the leading edge, such that spatiotemporally patterned calcium flicker activity can orchestrate the complex turning behaviour of migrating cells (Fig. 5e). The coupling of TRPM7-mediated force-transducing calcium influx and local $Ins(1,4,5)P_3$-induced calcium release would make this an ideal system for locomotion in response to chemoattractants (Fig. 5e). The present finding may have general ramifications because growth cones of neurons turn away from the side at which the filopodia displays higher local calcium signals[23] and calcium influx is essential for maintaining the leading-edge structure and activity in macrophages[14]. As such, unveiling calcium flickers in migrating cells opens a new avenue to investigate how local calcium signals orchestrate diverse biochemical pathways in the guidance of directional movement.

METHODS SUMMARY

Human lung embryonic WI-38 fibroblasts were obtained from the American Type Culture Collection and were loaded with Fluo-4 AM alone or in combination with Fura red AM. Images were captured on a Zeiss LSM 510 confocal microscope. The primers used for PCR with reverse transcription (RT–PCR) or quantitative RT–PCR are shown in Supplementary Table 1. Short interfering RNA (siRNA) sequences and scrambled controls were designed using RNAi Designer (http://www.invitrogen.com/rnai; Supplementary Table 2). WI-38 fibroblasts were transfected with 100 nM siRNA duplexes using Lipofectamine RNAiMax (Invitrogen) according to the manufacturer's recommendations. Western blotting or functional studies were carried out 72 h after transfection. Fibroblasts with an overt leading lamella and a thin trailing edge were selected for the cell-turning study. A PDGF-BB-containing micropipette was placed ~150 μm away from one side of the cell to establish a PDGF-BB gradient. Twenty-four-well Transwell plates (Corning) were used for the chemotaxis assay. The outer wells contained 0.8 nM PDGF-BB and overnight-starved WI-38 fibroblasts in PDGF-BB-free medium. Designated drugs were added to the inserts. For the assay, cells were loaded with calcein AM and then fixed immediately with formaldehyde. Cells under the lower surface of the polycarbonate membrane were imaged and analysed. For electrophysiological measurements, the cell-attached patch-clamp technique, using an EPC-7 amplifier, was applied to fibroblasts preloaded with Fluo-4 AM. To activate SACCs, mechanical suction of ~40 mm Hg was applied by means of a syringe connected to the patch pipette. In the mechanical perturbation experiment, shear stress was locally applied by a gentle jet flow by means of a patch pipette ~80 μm from the front of migrating fibroblasts. Digital image processing used IDL software (Research Systems) and custom-devised computer algorithms. Statistical data are expressed as mean and s.e.m. Student's *t*-test and paired *t*-test were applied when appropriate.

Full Methods and any associated references are available in the online version of the paper at www.nature.com/nature.

Received 13 April; accepted 21 October 2008.
Published online 31 December 2008.

1. Ridley, A. J. *et al.* Cell migration: integrating signals from front to back. *Science* **302,** 1704–1709 (2003).
2. Martin, P. & Parkhurst, S. M. Parallels between tissue repair and embryo morphogenesis. *Development* **131,** 3021–3034 (2004).
3. Werner, S. & Grose, R. Regulation of wound healing by growth factors and cytokines. *Physiol. Rev.* **83,** 835–870 (2003).
4. Van Haastert, P. J. & Devreotes, P. N. Chemotaxis: signalling the way forward. *Nature Rev. Mol. Cell Biol.* **5,** 626–634 (2004).
5. Pettit, E. J. & Fay, F. S. Cytosolic free calcium and the cytoskeleton in the control of leukocyte chemotaxis. *Physiol. Rev.* **78,** 949–967 (1998).
6. Brundage, R. A., Fogarty, K. E., Tuft, R. A. & Fay, F. S. Calcium gradients underlying polarization and chemotaxis of eosinophils. *Science* **254,** 703–706 (1991).
7. Lee, J., Ishihara, A., Oxford, G., Johnson, B. & Jacobson, K. Regulation of cell movement is mediated by stretch-activated calcium channels. *Nature* **400,** 382–386 (1999).
8. Nilius, B., Owsianik, G., Voets, T. & Peters, J. A. Transient receptor potential cation channels in disease. *Physiol. Rev.* **87,** 165–217 (2007).
9. Hahn, K., DeBiasio, R. & Taylor, D. L. Patterns of elevated free calcium and calmodulin activation in living cells. *Nature* **359,** 736–738 (1992).
10. Stossel, T. P., Fenteany, G. & Hartwig, J. H. Cell surface actin remodeling. *J. Cell Sci.* **119,** 3261–3264 (2006).
11. Robinson, R. C. *et al.* Domain movement in gelsolin: a calcium-activated switch. *Science* **286,** 1939–1942 (1999).
12. Chew, T. L., Wolf, W. A., Gallagher, P. J., Matsumura, F. & Chisholm, R. L. A fluorescent resonant energy transfer-based biosensor reveals transient and regional myosin light chain kinase activation in lamella and cleavage furrows. *J. Cell Biol.* **156,** 543–553 (2002).
13. Franco, S. J. *et al.* Calpain-mediated proteolysis of talin regulates adhesion dynamics. *Nature Cell Biol.* **6,** 977–983 (2004).
14. Evans, J. H. & Falke, J. J. Ca^{2+} influx is an essential component of the positive-feedback loop that maintains leading-edge structure and activity in macrophages. *Proc. Natl Acad. Sci. USA* **104,** 16176–16181 (2007).
15. Cheng, H. & Lederer, W. J. Calcium sparks. *Physiol. Rev.* **88,** 1491–1545 (2008).
16. Hamill, O. P. & McBride, D. W. Jr. The pharmacology of mechanogated membrane ion channels. *Pharmacol. Rev.* **48,** 231–252 (1996).
17. Zou, H., Lifshitz, L. M., Tuft, R. A., Fogarty, K. E. & Singer, J. J. Visualization of Ca^{2+} entry through single stretch-activated cation channels. *Proc. Natl Acad. Sci. USA* **99,** 6404–6409 (2002).
18. Numata, T., Shimizu, T. & Okada, Y. TRPM7 is a stretch- and swelling-activated cation channel involved in volume regulation in human epithelial cells. *Am. J. Physiol. Cell Physiol.* **292,** C460–C467 (2007).
19. Thomas, D. *et al.* Microscopic properties of elementary Ca^{2+} release sites in non-excitable cells. *Curr. Biol.* **10,** 8–15 (2000).
20. Patterson, R. L., Boehning, D. & Snyder, S. H. Inositol 1,4,5-trisphosphate receptors as signal integrators. *Annu. Rev. Biochem.* **73,** 437–465 (2004).
21. Horwitz, A. R. & Parsons, J. T. Cell migration—movin' on. *Science* **286,** 1102–1103 (1999).
22. Pierschbacher, M. D. & Ruoslahti, E. Cell attachment activity of fibronectin can be duplicated by small synthetic fragments of the molecule. *Nature* **309,** 30–33 (1984).
23. Gomez, T. M., Robles, E., Poo, M. & Spitzer, N. C. Filopodial calcium transients promote substrate-dependent growth cone turning. *Science* **291,** 1983–1987 (2001).
24. Shu, S., Liu, X. & Korn, E. D. Blebbistatin and blebbistatin-inactivated myosin II inhibit myosin II-independent processes in Dictyostelium. *Proc. Natl Acad. Sci. USA* **102,** 1472–1477 (2005).
25. Price, L. S. *et al.* Calcium signaling regulates translocation and activation of Rac. *J. Biol. Chem.* **278,** 39413–39421 (2003).
26. Weiner, O. D. *et al.* A $PtdInsP_3$- and Rho GTPase-mediated positive feedback loop regulates neutrophil polarity. *Nature Cell Biol.* **4,** 509–513 (2002).
27. van Haastert, P. J., Keizer-Gunnink, I. & Kortholt, A. Essential role of PI3-kinase and phospholipase A2 in *Dictyostelium discoideum* chemotaxis. *J. Cell Biol.* **177,** 809–816 (2007).
28. Hawkins, P. T. *et al.* PDGF stimulates an increase in GTP–Rac via activation of phosphoinositide 3-kinase. *Curr. Biol.* **5,** 393–403 (1995).
29. Claesson-Welsh, L. Platelet-derived growth factor receptor signals. *J. Biol. Chem.* **269,** 32023–32026 (1994).
30. Ware, M. F., Wells, A. & Lauffenburger, D. A. Epidermal growth factor alters fibroblast migration speed and directional persistence reciprocally and in a matrix-dependent manner. *J. Cell Sci.* **111,** 2423–2432 (1998).

Supplementary Information is linked to the online version of the paper at www.nature.com/nature.

Acknowledgements We thank I. C. Bruce, X. Zhu, J. J. Ma, H. Q. Cao, J. Liu, M. Zheng, X. D. Fu and R. P. Xiao for discussions, and M. Gorospe, Z. C. Liang, Q. Du, C. M. Cao, H. Huang, X. M. Lan, N. Lin, Y. R. Wang, R. S. Song and Y. Zhang for technical support. Special thanks to X. D. Fu for making his laboratory facility available to us. This work was supported by the Major State Basic Research Development Program of China (2007CB512100), and the National Natural Science Foundation of China (30630021 and 30800371) and an NIH grant (HL090905).

Author Information Reprints and permissions information is available at www.nature.com/reprints. Correspondence and requests for materials should be addressed to H.C. (chengp@pku.edu.cn) and C.W. (chaoliang.wei@gmail.com).

©2009 Macmillan Publishers Limited. All rights reserved

METHODS

Cell culture. Human lung embryonic WI-38 fibroblasts (21 population doublings) obtained from the American Type Culture Collection were maintained and subcultured to 28 population doublings in MEM (Gibco) supplemented with 10% FBS (Hyclone), 2 mM glutamine and 200 units ml^{-1} penicillin in a incubator with parameters preset at 37 °C and 5% CO_2. For functional experiments, cells were plated at a density of 1×10^4 per cm^2 and cultured for 10 h on coverslips coated with 5 μg ml^{-1} fibronectin (Sigma).

Calcium imaging. WI-38 cells were loaded with Fluo-4 AM (5 μM) alone or in combination with Fura red AM (5 μM) for 6 min at 37 °C, rinsed twice, and then bathed in HEPES-buffered saline solution containing (in mM): 134 NaCl, 5.4 KCl, 1.0 $MgSO_4$, 1.0 NaH_2PO_4, 1.8 $CaCl_2$, 20 HEPES and 5 D-glucose (pH 7.4) with 1% FBS, unless otherwise specified. Cells were placed in a 37 °C heated chamber (Zeiss S-Type incubator) and imaged on a Zeiss LSM 510 confocal microscope with a ×40 oil objective (NA 1.3) at radial and axial resolutions of 0.4 μm and 1.0 μm, respectively. For ratiometric imaging, cells were excited at 488 nm, emission was detected at 505–550 nm (Fluo-4 signal) and >633 nm (Fura red signal), and the differential interference contrast transmission image was acquired simultaneously. For migration path analysis and calcium flicker signal mass measurements, 300–600 time-lapse images were acquired at 6-s intervals. High-resolution linescan imaging of calcium flickers was performed at 3 ms per linescan.

PCR. Total RNA was isolated from WI-38 fibroblasts (28 population doublings) with TRI Reagent (Sigma) and converted to complementary DNA using M-MLV reverse transcriptase (Promega). Quantitative RT–PCR reactions were carried out using these cDNAs in an iQ5 real-time PCR detection system (BioRad). Results were read out using iQ5 optical system software. All samples showing primer dimer formation or spurious, non-specific peaks, as indicated by the dissociation curve, were excluded from analysis. The primers are shown in Supplementary Table 1.

RNA interference. RNAi sequences for Ins(1,4,5)P_3R isoforms and TRP channels were designed using RNAi Designer (http://www.invitrogen.com/rnai; Supplementary Table 2). Each scrambled control was designed corresponding to first duplex of siRNA. In brief, corresponding siRNA duplexes were synthesized (GenePharma or Invitrogen) and transfected into cells with Lipofectamine RNAiMax (Invitrogen) according to the manufacturer's recommendations. Western blotting or functional studies were carried out 72 h after transfection.

Western blotting. Total protein extracted from WI-38 cells with siRNA treatment was separated on 4–12% NuPAGE Novex Bis-Tris gels (Invitrogen) and transferred to PVDF membranes (Millipore). After blocking for 1 h with 5% non-fat dry milk, the PVDF membrane was probed with primary antibody (anti-Ins(1,4,5)P_3R2 was the gift of J. Chen; anti-Ins(1,4,5)P_3R3 was from Santa Cruz; anti-tubulin from Sigma; anti-TRPC6 from Millipore; anti-TRPV2 from ABR; and anti-PKD2 and anti-TRPM7 from Abcam) for 2 h at room temperature (20–25 °C), and then secondary antibody (IRDye-conjugated anti-mouse, anti-rabbit and anti-goat IgG from LI-COR) for 1 h at room temperature. Immunoblots were detected using the Odyssey imaging system.

Cell migration analysis. Fibroblasts with an overt leading lamella and a thin trailing edge were selected for migration analysis. The outer boundary of the cell was extracted from the respective fluorescence image for calculation of its centre of gravity. The centres of consecutive images (6 s apart) defined the trajectory of cell movement. Migration speed was calculated as the average displacement per min during 30 min. Directional persistence (D/T ratio) was calculated as the ratio between the linear displacement and the total length of the trajectory during 30 min.

To establish a PDGF-BB (PeproTech) gradient perpendicular to the long axis of a polarized migrating fibroblast, a 5 μm internal diameter, PDGF-BB-containing (3 nM) micropipette was placed ~150 μm away from one side of the cell. By visualization of sulphurhodamine fluorescence under similar conditions, we estimated an average PDGF concentration of 1 nM and an edge-to-edge difference of 0.4 nM across the leading lamella (~40 μm).

Chemotaxis assay. Twenty-four-well Transwell plates with inserts containing 8-μm pores in a polycarbonate membrane (Corning) were used for the chemotaxis assays. In brief, the outer wells contained 600 μl MEM medium containing 1% FBS with PDGF-BB (0.8 nM) as a chemoattractant. Approximately 8×10^3 overnight-starved (1% FBS) WI-38 fibroblasts in 100 μl PDGF-BB-free MEM medium containing 1% FBS and designated drug were added to each insert. In the chemokinesis control group, PDGF-BB (0.8 nM) was also added to the insert to abolish the concentration gradient. Transwell plate was then incubated for 12 h in an incubator with parameters preset at 37 °C and 5% CO_2 before assay.

For the assay, the inserts were loaded with 5 μM calcein AM for 10 min and then fixed immediately with 3% formaldehyde for 10 min. Cells in inserts were cleared and those under the lower surface of the polycarbonate membrane were imaged and analysed.

Application of mechanical forces. Shear stress was locally applied by a gentle jet flow (4 cm H_2O pressure) by means of a patch pipette (10 μm internal diameter) ~80 μm away from the front of migrating fibroblasts. Note that jet flow used in local drug delivery (1 cm H_2O pressure, ~120 μm placement, pipette with 5 μm internal diameter) did not alter calcium flicker activity ($n = 4$).

Recording SACC currents and imaging local calcium influx. Cell-attached patch-clamp technique, using an EPC-7 amplifier, was applied to fibroblasts preloaded with the calcium indicator, Fluo-4 AM. The patch pipette (2–3 MΩ) solution contained (in mM): NaCl 140, KCl 5.4, $MgCl_2$ 1.0, HEPES 20 and $CaCl_2$ 1.8 (pH 7.4, adjusted with NaOH). To activate SACCs, mechanical suction of ~40 mm Hg was applied by means of a syringe connected to the patch pipette while the patch membrane was held 80 mV more negative than the resting membrane potential to enhance Ca^{2+} entry. The single-channel currents were filtered at 3 kHz and digitised at 5 kHz with pClamp 6.0 software. Linescan images of local calcium immediately beneath the patch membrane were acquired simultaneously at 3 ms resolution.

Data analysis. Digital image processing used IDL software (Research Systems) and custom-devised computer algorithms. Statistical data are expressed as mean and s.e.m. Student's t-test and paired t-test were applied when appropriate. A P value less than 0.05 was considered as statistically significant.

©2009 Macmillan Publishers Limited. All rights reserved